RESEARCH PAPER

Bulk and compound-specific δ^{13}C and *n*-alkane indices in a palustrine intermontane record for assessing environmental changes over the past 320 ka: the Padul Basin (Southwestern Mediterranean realm)

José E. Ortiz[1] · Trinidad Torres[1] · Antonio Delgado[2] · Maruja Valle[3] · Vicente Soler[4] · Rafael Araujo[5] · María R. Rivas[3] · Ramón Julià[6] · Yolanda Sánchez-Palencia[1] · Rogelio Vega-Panizo[1]

Abstract

Here we provide valuable information about the palaeoenvironmental evolution of Southwestern Mediterranean region during the last ca. 320 ka through a biomarker-based study of the longest continuous continental Quaternary record in the Iberian Peninsula. The *n*-alkane content and δ^{13}C values of these lipids were measured in 300 samples taken from the uppermost 55 m of the Padul Basin (PB) record. The δ^{13}C signal of long-chain *n*-alkanes was a reliable proxy for C_4/C_3 terrestrial vegetation composition in the basin, as emergent macrophytes made a minor contribution to these homologues. In contrast, the δ^{13}C values of C_{23} and C_{25} alkanes reflected mainly phases of increasing water level of the lacustrine/palustrine water body since aquatic macrophytes contain a large proportion of these compounds. Low δ^{13}C values were attributed to a marked contribution of plants using the C_3 photosynthetic pathway. Intervals with the lowest δ^{13}C values were attributed to an important input of angiosperms, although they could also be explained by changing environmental conditions or environmental stress, as large shifts in δ^{13}C occurred in long-chain homologues typically abundant in terrestrial plants. Shifts in δ^{13}C of medium-chain homologues reflected limited CO_2 availability induced by water temperature, salinity, pH, enhanced productivity, low atmospheric pCO2, or stagnant barriers, rather than the abundance of aquatic macrophytes. Our results also suggest enhanced isotopic fractionation during lipid synthesis by aquatic macrophytes within MIS 7 and the Holocene, leading to increased δ^{13}C values of bulk OM and of long-chain *n*-alkanes. Hence, the δ^{13}C logs were ideal for studying the contribution of aquatic macrophytes to the lipid and isotopic composition of sediments and for the reconstruction of palaeoenvironmental conditions. These results confirmed that C_4 plants had a low presence in the PB. Comparison with biomarker analysis and pollen data of the PB and other records of the Southwestern Mediterranean revealed that δ^{13}C values of bulk OM and of long-chain *n*-alkanes reflected global climatic oscillations during MIS 7 and the episodes Heinrich Events 3, 2, 1 and Younger Dryas.

Keywords *n*-alkanes · δ^{13}C · Aquatic plants · Terrestrial plants · Padul · Palaeoenvironment

✉ José E. Ortiz
joseeugenio.ortiz@upm.es

1 Laboratory of Biomolecular Stratigraphy, E.T.S.I. Minas Y Energía, Universidad Politécnica de Madrid, C/ Ríos Rosas 21, 28003 Madrid, Spain

2 Laboratorio de Biogeoquímica de Isótopos Estables, Instituto Andaluz de Ciencias de La Tierra (CSIC), Avda. de Las Palmeras, 4, Armilla, 18100 Granada, Spain

3 Facultad de Ciencias, Universidad de Salamanca. Pza de La Merced S/N, 37008 Salamanca, Spain

4 Instituto de Agrobiología Y Productos Naturales (C.S.I.C.), Avda Astrofísico Fco Sánchez 3, La Laguna, 38206 Tenerife, Spain

5 Museo Nacional de Ciencias Naturales (CSIC), C/ José Gutiérrez Abascal 2, 28006 Madrid, Spain

6 Instituto de Ciencias de La Tierra "Jaume Almera" (C.S.I.C.), C/ Lluís Solé I Sabarís S/N, 08028 Barcelona, Spain

Resumen

Proporcionamos información valiosa sobre la evolución paleoambiental de la región Mediterráneo suroccidental durante los últimos ca. 320 ka a través del estudio de biomarcadores del registro continental continuo Cuaternario más largo de la Península Ibérica. El contenido de n-alcanos y los valores de $\delta^{13}C$ de estos lípidos se midieron en 300 muestras tomadas de los 55 m superiores del registro de la cuenca de Padul. La señal $\delta^{13}C$ de los *n*-alcanos de cadena larga proporcionó información sobre la vegetación terrestre C_4/C_3 en la cuenca, ya que las macrofitas emergentes contribuyen en menor grado a la señal de estos compuestos de mayor peso molecular. Por el contrario, los valores de $\delta^{13}C$ de los alcanos C_{23} y C_{25} reflejaron, principalmente, fases de aumento del nivel de agua, ya que las macrofitas acuáticas contienen una gran proporción de estos compuestos. Los valores bajos de $\delta^{13}C$ se atribuyeron a una marcada contribución de las plantas que utilizan la vía fotosintética C_3. Los intervalos con los valores más bajos de $\delta^{13}C$ se atribuyeron a un aporte importante de angiospermas, aunque también podrían explicarse por condiciones ambientales cambiantes o estrés ambiental, ya que se produjeron grandes cambios en $\delta^{13}C$ en alcanos de cadena larga típicamente abundantes en plantas terrestres. Los cambios en $\delta^{13}C$ de los alcanos de cadena media reflejaron la disponibilidad limitada de CO_2 inducida por la temperatura del agua, la salinidad, el pH, la productividad mejorada, la pCO_2 atmosférica baja o las barreras estancadas, en lugar de la abundancia de macrofitas acuáticas. Los resultados también sugieren un mayor fraccionamiento isotópico durante la síntesis de lípidos por parte de macrofitas acuáticas en el MIS 7 y Holoceno, lo que produjo un aumento de los valores de $\delta^{13}C$ en la materia orgánica y en los n-alcanos de cadena larga. Por lo tanto, el registro de $\delta^{13}C$ resultó fundamental para determinar la contribución de las macrofitas acuáticas a la composición lipídica e isotópica de la materia orgánica de los sedimentos y la reconstrucción paleoambiental. Estos resultados confirmaron que las plantas C4 contribuyeron de manera muy limitada al registro de la Cuenca del Padul. La comparación de estos resultados con el análisis de biomarcadores y polínico de la cuenca de Padul, así como con otros registros del suroeste del Mediterráneo reveló que $\delta^{13}C$ de la materia orgánica y de los alcanos de cadena larga reflejaron las oscilaciones climáticas globales del MIS 7, los Eventos Heinrich 3, 2, 1 y Younger Dryas.

Palabras clave *n*-alcanos · $\delta^{13}C$ · Plantas acuáticas · Plantas terrestres · Padul · Paleoambiente

1 Introduction

Lacustrine and palustrine sediments provide excellent palaeoclimatic and palaeoenvironmental reconstructions from the study of a variety of proxies, including elemental, isotopic and molecular organic geochemical ones. Among these, biomarkers are commonly used to reconstruct past environmental conditions (Meyers 1997, 2003; Meyers and Ishiwatari 1993; Ortiz et al. 2010; Xie et al. 2004; Zhou et al. 2005, among others). In particular, *n*-alkanes have been extensively used for this purpose. The sources of *n*-alkanes in geological records can be inferred from their molecular distributions. The *n*-alkanes of the leaf wax of terrestrial plants are enriched in C_{27} to C_{31}, whereas aquatic macrophytes are characterized by the predominance of C_{23} and C_{25} homologues (Eglinton and Hamilton 1963, 1967). Short-chain *n*-alkanes (C_{17} and C_{19}) are attributed mainly to algae and cyanobacteria (Cranwell et al. 1987). Given these considerations, indexes like the average chain length (ACL) (Poynter 1989) have been developed to estimate the contribution of different types of vegetation to sediments. In this regard, the aquatic macrophyte proxy (*P*aq) (Ficken et al. 2000) provides information about the input of aquatic macrophytes to marine, lacustrine and palustrine environments.

The carbon isotopic composition of organic matter (OM) in lake sediments is widely used in palaeolimnology. $\delta^{13}C$ values can be used for studying changes in bulk OM sources (mainly C_3 and C_4 vegetation), for reconstructing palaeoenvironmental conditions (Farquhar et al. 1989; Ficken et al. 1998; Street-Perrot et al. 2004; Eley et al. 2016, among others) and past productivity rates (e.g., Brenner et al. 1999; Hodell and Schelske 1998; Hollander and McKenzie 1991; Hollander et al. 1992; Meyers 2003), and for identifying changes in nutrient availability in surface waters (Bernasconi et al. 1997; Teranes and Bernasconi 2005). In this regard, the distinct CO_2 fixation pathways of plants produce characteristic differences in the stable carbon isotope composition of leaf waxes, with C_3 plants usually having more depleted $\delta^{13}C$ values than C_4 plants, which in turn are related to climatic characteristics, as the abundance of the latter shows good correspondence with arid conditions. Similarly, phytoplankton (C_3 algae) preferentially utilize ^{12}C to produce OM, which is approximately $20^0/_{00}$ lighter than the $^{13}C/^{12}C$ ratio of their dissolved inorganic carbon (DIC) source (cf., O'Leary 1988; Wolfe et al. 2001), and this proxy can be used to estimate productivity.

The $\delta^{13}C$ composition of specific compounds has been employed in recent years for palaeoenvironmental interpretations. The $\delta^{13}C$ composition of individual *n*-alkanes has been used to infer biosynthetic processes, source inputs, and palaeoenvironmental conditions, and it provides more specific data on past changes in C_3 and C_4 plant abundance than the $\delta^{13}C$ of bulk OM (Street-Perrot et al. 1997; Ficken et al. 1998; Huang et al. 2000, 2001; Sinninghe Damsté et al.

2011; Sun et al. 2013). Thus, the $\delta^{13}C$ values of long-chain *n*-alkanes, which are derived mainly from terrestrial vegetation, are used to reconstruct the input of OM from C_3 and C_4 plants to sediments (Ficken et al. 1998; Huang et al. 2001, 2006; Liu et al. 2015; Sinninghe Damsté et al. 2011; Yamamoto et al. 2010). Changes in the contribution of C_3 and C_4 plants are controlled mainly by climatic and environmental factors, such as temperature, aridity and atmospheric CO_2 levels (Cerling et al. 1997; Huang et al. 2001), although other factors (e.g. pH, salinity, productivity) are likely to affect both the bulk OM and compound-specific $\delta^{13}C$ signals (Hollander and McKenzie 1991; Hollander et al. 1992; Meyers 2003; Street-Perrot et al. 2004; Eley et al. 2016).

Thus, the $\delta^{13}C$ composition of bulk OM and of long-chain *n*-alkanes in lake sediments has been traditionally considered a reliable way to track changes in the contribution of C_3 and C_4 plants. A key premise is that long-chain leaf wax components are derived primarily from land plants. However, the input of aquatic macrophytes can be underestimated (Liu et al. 2015). Moreover, the wide range of $\delta^{13}C$ values of medium- and some long-chain *n*-alkanes may bias the interpretation towards more C_3 or C_4 plants, as aquatic macrophytes show large variations in $\delta^{13}C$ values (Aichner et al. 2010; Liu et al. 2015).

Located in the south of the Iberian Peninsula, the Padul Basin (PB) has one of the longest terrestrial records in the world, the main one in the Southern Mediterranean realm, with more than 100 m covering ca. 1 Ma (Ortiz et al. 2004, 2010). The importance of the PB was first recognised in the pollen studies of Menéndez Amor and Florschütz (1962, 1964) and Florschütz et al. (1971) performed in a ca. 100-m deep core, and of Pons and Reille (1988) in a composite record of 22.8 m. In 1997, a 107 m-long core (SPD) was drilled where the basin reaches its maximum depth near its western edge (Nestares and Torres 1998). High resolution pollen and organic geochemistry studies from this watershed reveal changes in vegetation that can be attributed to alterations in climatic and environmental conditions in the Southern Mediterranean realm over ca. 1 Ma (Flörschutz et al. 1971; Pons et al. 1988; Ortiz et al. 2004, 2010; Torres et al. 2020). The record is characterized by an overwhelming presence of *Pinus*. The abundance of the typical steppe taxa *Artemisia* and Chenopodiaceae are linked to arid phases, while an increase in Mediterranean vegetation, deciduous trees and Poaceae plants is interpreted as the development of a Mediterranean-like climate (Torres et al. 2020). In contrast, periods with predominance of pteridophytes (ferns) and deciduous trees, which both arise in more humid conditions, are scarce in the record. Ramos-Román et al. (2018a) also provided a climate reconstruction of the PB for the last 4700 cal yr BP based of the pollen record of a core drilled in the western part of the basin. Ramos-Román et al. (2018b) reconstructed the vegetation and environmental conditions of the last ca. 11.6 cal ka BP by integrating pollen, inorganic and organic

geochemical and sedimentological analyses. Also, Camuera et al. (2019) provided the pollen record of the last 200 ka. However, the chronological model used by these authors should be considered with caution, as it was constructed using only 2 ages older than 50 ka (ca. 65 ka and ca. 120 ka, after the rejection of 3 ages), and using linear extrapolation with two different sediment rates beyond ca. 120 ka (Camuera et al. 2018).

Lithology and organic geochemical proxies reveal the existence of two main phases in the record: from 107 to 60 m (1 Ma to 400 ka), with lacustrine conditions, and in the upper 60 m (last 400 ka), with palustrine conditions (Ortiz et al. 2004). The relative abundance of high molecular weight (MW) *n*-alkanes shows good correspondence with these large palaeoclimatic periods.

Research using other palaeoclimatological proxies has continued over the years. In this regard, the concentration of organic carbon, the atomic H/C and C/N ratios, and $\delta^{13}C$ and CPI values of bulk OM have proven to be excellent proxies for the study of the palaeoclimatological and palaeohydrological evolution of the Padul peat bog (Ortiz et al. 2004). However, global climatic changes (glacials and interglacials), such as those occurring from *ca.* 170 to 25 ka B.P. (from meter 33.6 to 7), did not greatly affect these palaeoenvironmental proxies, the values of which show little variation. Ortiz et al. (2010) demonstrated that the relative percentages of high MW alkanes (C_{27}, C_{29} and C_{31}) are useful for reconstructing the palaeoenvironmental evolution of the PB.

In the present study, we re-examined the last ca. 320 ka (upper 55 m) of the palaeoclimatological record of the PB, focusing on new data, namely the stable carbon isotope composition of *n*-alkanes, and various indexes related to the *n*-alkane content (mainly the *n*-alkane predominant chain, ACL and *P*aq indexes). In fact, ACL, *P*aq and $\delta^{13}C$ have been used together to reconstruct the palaeoenvironmental conditions of lacustrine environments (Seki et al. 2010; Sun et al. 2013).

The objectives of this study were (1) to provide new insights into the vegetation and climate change in the Southern Mediterranean realm during the last 320 ka based on stable carbon isotopic measurements of biomarkers in the PB record, (2) to examine the variability in the carbon isotopic composition of the Padul record: bulk and compound-specific $\delta^{13}C$ signals, focusing on *n*-alkanes, and (3) to combine the information provided by $\delta^{13}C$ values and *n*-alkane proxies.

2 Geographical, geological and bioclimatological settings

The PB catchment has a total area of 44 km², while the present peat bog covers 4.6 km² and is located 720 m a.s.l. (Fig. 1). The western boundary of the basin is formed by the elevations of the Albuñuelas range (1000 m a.s.l), while the eastern one is the bald and craggy Sierra Nevada, which reaches its highest point at the Mulhacén peak (3482 m a.s.l.), only 20 km east of Padul village (Fig. 1). The northern boundary is a small elevation (Suspiro del Moro, 830 m a.s.l.) that divides the PB and the Granada depression. The southern boundary is defined by the Dúrcal river gorge.

The PB resembles a typical endorheic basin that is tectonically controlled (Alfaro et al. 2001): an alluvial fan system developed along its eastern border, grading into

Fig. 1 A Geographical setting and panoramic view of the Padul Basin with the location of the main faults and alluvial fans. **B** Geological map of Padul (modified from Sanz de Galdeano 1996)

the lacustrine-palustrine environment. The still active Padul fault provides continuous subsidence at the western footwall of the basin, and the alluvial fan apices are aligned along the fault trace at 800–900 m a.s.l. (Alfaro et al. 2001) (Fig. 2). A maximum thickness of ca. 110 m is reached towards the eastern boundary of the basin, with Pleistocene sediments overlying Miocene marine ones. A dominant groundwater regime controls the hydrology of the basin, with a hydrogeological connection between the karst rock of Sierra Nevada and the PB itself, the run-off input of water being estimated to contribute only about 8% of the total (Cañada 1984).

The climate in the basin is Mediterranean with a continental influence. Winters are cold and dry, while summers are extremely hot, with maximum temperatures over 40 ℃. The average annual rainfall ranges from 400 to 450 mm yr⁻¹, evapotranspiration is 700–900 mm yr⁻¹, and the mean annual temperature is between 15 and 16 ℃ (Rivas-Martínez and Rivas-Sáenz 2009).

The present day accumulation of organic matter in the PB is linked to semi-aquatic plants like *Phragmites australis*, helophytic species (*Typha angustifolia, Scirpus lacustris, Ranunculus repens, Lythrum junceum, Apium nodiflorum, Veronica anagallis-aquatica*), and other hygrophilous plants (*Cyperus longus, Juncus articulatus, Ranunculus trilobus, Scrophularia auriculata*) (Sánchez-Castillo and Morales-Torres 1981). Riparian representatives, such as *Populus* sp., *Salix* sp. and *Fraxinus* sp., among others, also appear on the banks of the bog. The Sierra Nevada Range holds a series of vegetation belts, the main contribution belonging to the meso-Mediterranean belt below 900 m (57% of current vegetation) (Rivas-Martínez 1987).

The chronology of the PB record was calculated through consistent numerical datings (¹⁴C, Th/U, amino acid racemization and palaeomagnetism) of SPD core (Ortiz et al. 2004; Torres et al. 2020) and using Bayesian age–depth modelling created with the Bayesian R-code package "Bacon 2.3.7" (Blaauw and Christen 2011).

3 Materials and methods

The drilling was performed by the Geological Service of Spain, using a ring with a conventional drill pipe and direct flow of bentonite-water mud. The stratigraphy of the Padul SPD core (Latitude: 37º01' 01'' N; Longitude: 3º36' 07'' W; Elevation: 714.20 m) is shown in Fig. 2. For more details see Ortiz et al. (2004) and Ortiz et al. (2010). Coarse detrital material was predominant in the lower part of the core (from 107 to 70 m), with some scarce peaty intervals, whereas peaty lutites were dominant between
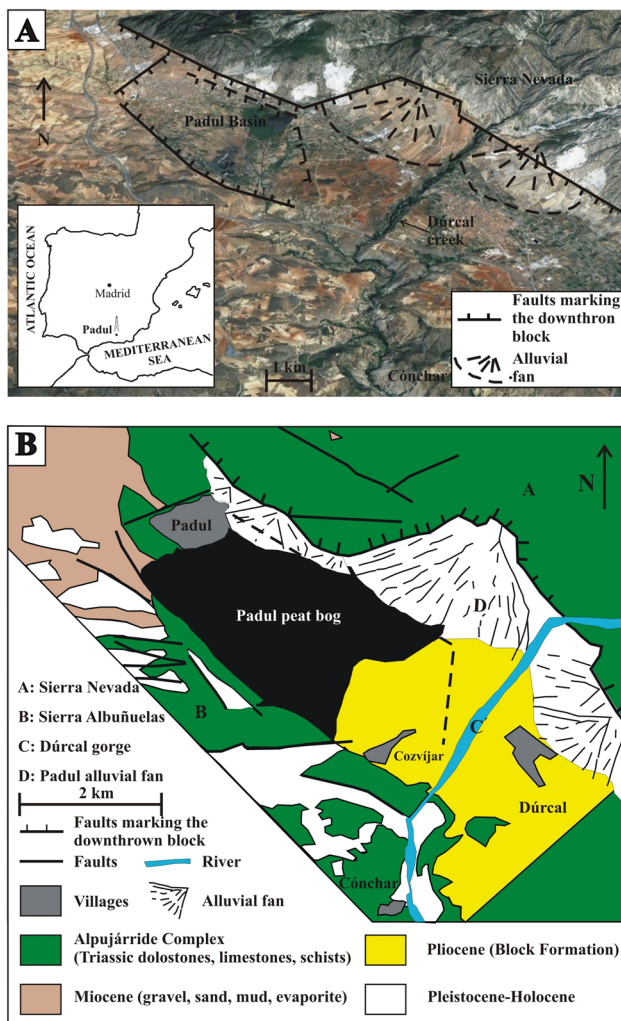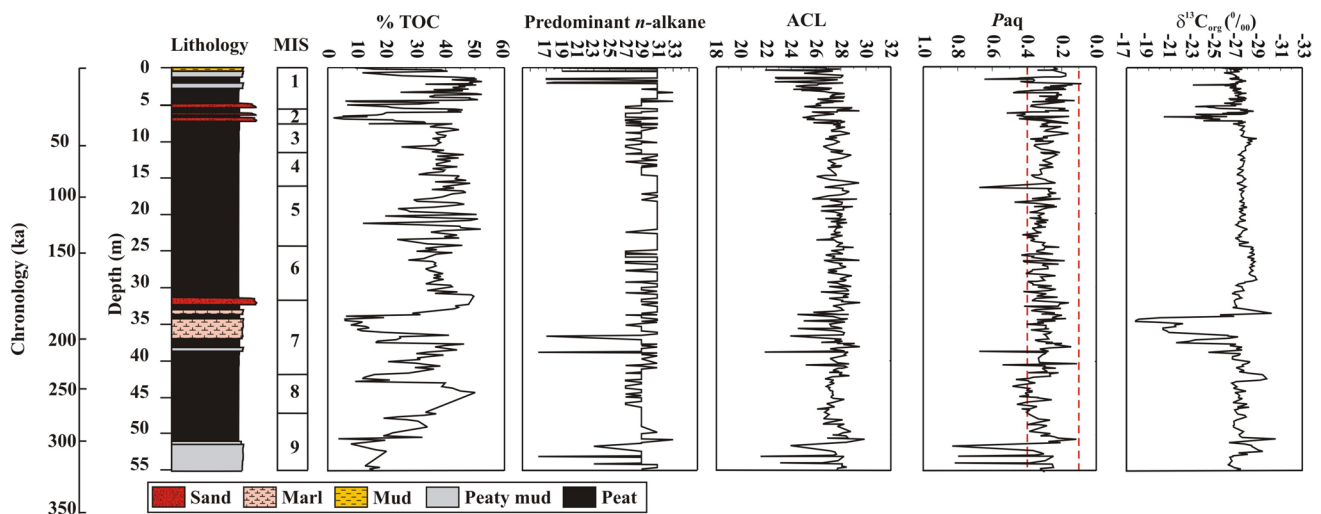
Fig. 2 Stratigraphy and chronology (Torres et al. 2020) of the upper 55 m of the Padul record, together with the profiles of the concentration of organic carbon (%TOC), bulk δ¹³C, predominant *n*-alkane chain, ACL, and *P*aq (Ortiz et al., 2004). The cut-off values for *P*aq (0.1; 0.4) were represented. Marine isotope stages (MIS) are also shown

70 and 50 m. In the uppermost 50 m, peat was abundant, with some marly (37–33 m) and sandy interbeds (7–5 m).

A total of 330 samples for lipid fraction and 270 samples for OM and *n*-alkane stable carbon isotope analysis were taken at approximately 15 to 20 cm intervals along the upper 55 m of the core.

3.1 Lipid extraction and analysis (biomarker analysis)

About 5–10 g of sediment was ground, and biomarkers were extracted following the LEB protocol (Lucini et al. 2000). Briefly, this procedure consists of a 24-h soxhlet extraction with dichloromethane and methanol 2:1 (suprasolv Merck) and concentration of the isolated bitumen using a rotor-vapor device. Three bitumen fractions were extracted through liquid chromatography in a silica-alumina glass column using solvents of distinct polarity, namely *n*-hexane, dichloromethane/*n*-hexane 4:1 and methanol. Samples were injected into an HP 6890 gas chromatograph equipped with a selective mass detector (HP 5973) and an ATM-5 column (250×0.25 mm; 0.20 µm). Helium was used as the carrier gas. The oven temperature was programmed from 60 to 300 ℃ at 6℃/min (holding time 20 min). The injector was programmed at 275℃. The compounds were identified using the Data Analysis Program and the Wiley Library. *n*-Alkanes were calculated from the GC/MS chromatograms of mass/charge *m/z* 57 from the first bitumen fraction (extracted with *n*-hexane), and decafluorobiphenyl was used as an internal standard.

3.2 Bulk organic matter δ¹³C analysis

Carbon isotope ratios of bulk OM were calculated at the "Estación Experimental El Zaidín". After carbonate removal with 1:1 HCl, the δ¹³C values of OM were measured in selected samples by means of an EA-IRMS elemental analyser connected to a Finnigan MAT 251 mass spectrometer. Results are expressed in δ-notation ($^0/_{00}$), using the international Vienna Pee Dee Belemnite (PDB) standard. The standard deviations are 0.1 $^0/_{00}$ for δ¹³C in OM.

3.3 Compound-specific δ¹³C analysis

Compound-specific δ¹³C analyses were performed on the aliphatic fraction (extracted with hexane) using a TraceGC Ultra (Thermo-Finnigan) gas chromatograph coupled to a Delta XP isotope ratio mass spectrometer (IRMS) at the "Estación Experimental El Zaidín". We used an ATM-5 column (250×0.25 mm; 0.20 µm). Helium was the carrier gas. The oven temperature was programmed from 60 to 300 ℃ (held 20 min) at 3℃/min. Carbon isotope ratios are expressed relative to the PDB standard. The reproducibility for replicate analysis is 0.1$^0/_{00}$.
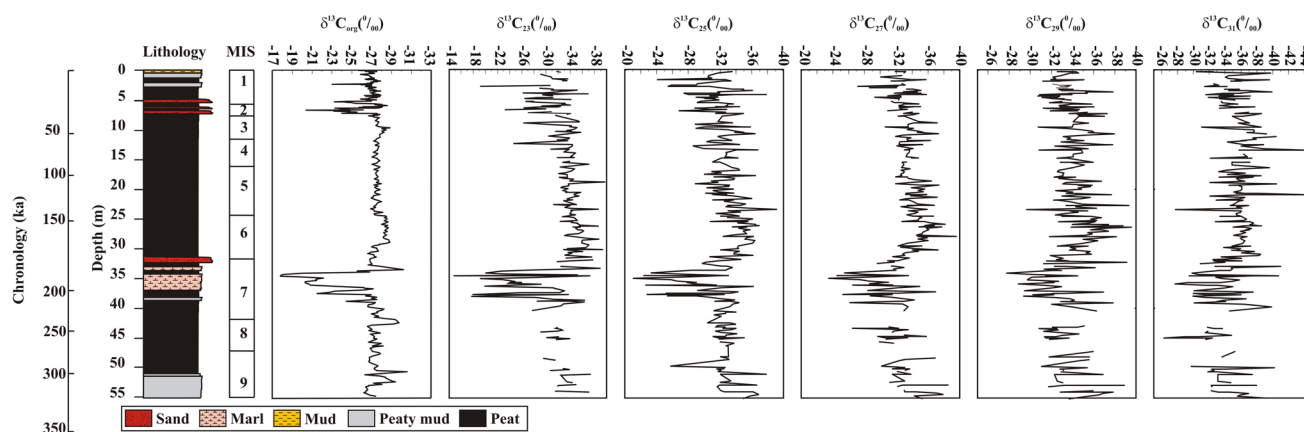
Fig. 3 Profiles of δ^{13}C values of bulk and even n-alkanes from C_{23} to C_{33} in the uppermost 55 m of the Padul record, together with the stratigraphy, chronology (Torres et al. 2020) and MIS

4 Results

The logs of the palaeoenvironmental proxies used in this study, i.e. concentration of total organic carbon (%TOC), diverse n-alkane indices, bulk δ^{13}C values, and δ^{13}C values of some n-alkanes, are shown in Figs. 2, 3.

The %TOC values were between 52.38 and 0.06. From a general point of view, the %TOC values showed oscillations, although most were between 30 and 55%. There were, however, some minima in the %TOC, which correlated with horizons consisting of marls (37–34 m) and sands (4 beds between 8 and 4.5 m). Of note, two other minima occurred at 52–51 m and 43–42 m.

4.1 n-Alkanes

All the samples showed an odd-over-even carbon number predominance (CPI values were higher than 2; Ortiz et al. 2004), with a chain-length distribution ranging mainly from C_{15} or C_{17} to C_{33} or C_{35}, maximizing either at low MW (C_{17} or C_{19}; Fig. 3) or long-chain alkanes (C_{27}, C_{29} and C_{31}), the former group predominant in only a few samples (Fig. 3).

The profiles of the n-alkane predominant chain, ACL and Paq indexes were considered. The Paq index, calculated as the $(C_{23} + C_{25})/(C_{23} + C_{25} + C_{29} + C_{31})$ ratio (Ficken et al. 2000), was postulated to reflect the relative contribution of emergent and submerged/floating aquatic macrophytes, which typically maximize at C_{23} and C_{25}, and of terrigenous plants. Paq values ranged between 0.08 (2.27 m) and 0.83 (51.50 m).

The ACL index (Poynter 1989), calculated as $[(C_i \times i + C_{i+1} \times (i+1) + C_{i+2} \times (i+2)... + C_n \times n))/ (\Sigma C_{n+1} + C_{n+2} + ... + C_n)$, with i = 13, n = 33], is a good proxy for distinguishing between the predominance of low vs. high MW n-alkanes (Pancost et al. 2002; Rommerskirschen et al. 2003). Most ACL values fell between 26.0 and 29.5,

with four marked intervals, namely 54–51 m (320–300 ka), 39–34 m (220–180 ka), 7–5 m (25–15 cal ka BP) and upper 2.5 m (7.5 cal ka BP), with lower values coinciding with a dominance of short- to medium-chain n-alkanes.

4.2 δ^{13}C values

The δ^{13}C values of bulk OM ranged between -31.46 and -17.83 $^0/_{00}$ They did not show marked oscillations, with most of the samples ranging between -27.0 and $-29.0^0/_{00}$, with the exception between 39 and 34 m (220–180 ka), which showed a shift to less negative values, and in the upper 7 m, in which some samples provided values over -26.0 $^0/_{00}$.

The stable carbon isotopic composition of n-alkanes varied substantially. C_{31} and C_{33} n-alkanes were typically the most depleted and they ranged from $-26.2^0/_{00}$ to as much as $-46.6^0/_{00}$, with the latter showing the most depleted values. δ^{13}C values for C_{29} oscillated between -27.7 and $-39.6^0/_{00}$ and for C_{27} between -23.5 and $-39.6^0/_{00}$.

In contrast, the δ^{13}C for C_{23} and C_{25} showed values as low as $-14.8^0/_{00}$ and $-20.9^0/_{00}$, respectively between 39 and 34 m (220–180 ka). Some samples of the uppermost 7 m also showed less negative δ^{13}C values. The most depleted values were $-40.3^0/_{00}$ and $-39.2^0/_{00}$, respectively.

5 Discussion

5.1 Origin of n-alkanes

n-Alkane profiles were used to distinguish the diverse sources of OM, namely algal, aquatic or terrigenous. Each sample can be characterized by the predominant n-alkane chain length. Phytoplankton and algae are dominated by low MW n-alkanes, maximizing at C_{17} (Blumer et al. 1971;

Cranwell et al. [1987]; Gelpi et al. [1970]). Submerged/floating macrophytes maximize at C_{21}, C_{23} and C_{25} (Cranwell [1984]; Ogura et al. [1990]; Viso et al. [1993]), while emergent macrophytes have a composition similar to that of terrestrial plants, peaking at C_{27} and C_{29} (Cranwell [1984]). Land plants contain a high proportion of higher MW n-alkanes (C_{27}, C_{29} and C_{31}) in their epicuticular wax (Cranwell et al. [1987]; Eglinton and Calvin [1967]; Eglinton and Hamilton [1963], [1967]; Nott et al. [2000]; Pancost et al. [2002]; Rieley et al. [1991]). Deciduous trees typically maximize at C_{27}, whereas C_{31} is dominant in marsh plants and possibly grasses (Cranwell et al. [1987]; Ortiz et al. [2004], [2010]; Schwark et al. [2002]). However, data from a broad survey of modern plants show that n-alkane chain-length distributions are highly variable within plant groups, and chemotaxonomic distinctions between grasses and woody plants are difficult to make, with the exception of aquatic plants and *Sphagnum* moss (Bush and McInerney [2013]). In contrast, changes in chain length distribution are likely to be a result of temperature and/or humidity conditions (Bush and McInerney [2015]).

In the PB record, most of the samples from the upper part of the core maximized at C_{27}, C_{29} or C_{31} n-alkanes, while the C_{17} and C_{23} were predominant in some samples between 54 and 51 m (320–300 ka), 39 and 37 m (320–300 ka) and the upper 2.5 m (7.5 cal ka BP). Therefore, the n-alkanes present in the sediment probably derived from terrestrial plants, with some exceptions in which the C_{17} and C_{23} homologues were predominant, indicating a major input from algae and aquatic macrophytes, respectively. Samples in which C_{27} was the most abundant n-alkane might be also linked to aquatic macrophytes. Of note, a bimodal distribution was detected in some samples, with maxima at medium- and long-chain n-alkanes, thereby indicating the contribution of distinct types of OM: land plants and aquatic macrophytes.

The ACL index did not show significant oscillations, with values ranging between 29.5 and 27.0, confirming the major input of terrestrial plants. Only between 54 and 51 m (320–300 ka) and in the uppermost 2.5 m did ACL values fall below 25.0. This observation is attributed to an important contribution of algae and/or aquatic macrophytes. Of note, between 39 and 34 m (220–180 ka), and 7 and 4 m (25–10 cal ka BP), ACL values were between 27.0 and 25.0, indicating a significant input of aquatic macrophytes.

The Paq index reflected the abundance of emergent and submerged/floating aquatic macrophytes. According to Ficken et al. ([2000]), values < 0.1 are linked to a dominant contribution from land plants, while those between 0.1 and 0.4 indicate a significant input from emergent macrophytes. Values > 0.4 are typical in sediments with a major n-alkane input from submerged/floating macrophytes.

In the Padul record, most Paq values fell between 0.1 and 0.4. Therefore, although the predominant n-alkane chain and ACL values indicated a major input of land plants, the Paq index pointed to a considerable contribution of emergent macrophytes. Therefore, a mixed contribution of terrestrial plants and aquatic macrophytes occurred. It must also be highlighted that samples from between 54 and 51 m, and a few between 39 and 34 m (220–180 ka), 7 and 4 m (25–10 cal ka BP) and the upper 2.5 m (7.5 cal ka BP) registered Paq values over 0.4, thereby indicating a major input of submerged macrophytes, which is consistent with lower ACL values and the predominance of short-chain n-alkanes.

5.2 δ13C values

The isotopic proxies and n-alkane ratios provide a general overview of the palaeovegetation and palaeoenvironmental changes in the PB record. $\delta^{13}C$ values of bulk OM have been examined previously (Ortiz et al. [2004]), but here we widened the study by addressing compound-specific $\delta^{13}C$ signals and exploring the relationships with n-alkane proxies.

5.2.1 δ13C values of bulk OM

The carbon isotopic composition of OM ($\delta^{13}C$) in lake sediments is frequently used to distinguish the source of this material, especially between terrestrial and aquatic plants. It can further differentiate different types of land plants (C_3 and C_4) and can be used to constrain algal productivity (Talbot and Johannessen [1992]).

Thus, C_3 land plants (mainly trees, shrubs and cold climate grasses) commonly show $\delta^{13}C$ values between -23 and $-31^0/_{00}$ (O´Leary [1981], [1988]; Meyers [1990]; Collister et al. [1994]; Meyers et al. [1995]; Meyers and Lallier-Verges [1999]; Ficken et al. [2000]; Bi et al. [2005]), with a mean value of $-27^0/_{00}$. According to Diefendorf et al. ([2010]) and Chikaraishi and Naraoka ([2003]), $\delta^{13}C$ values in C_3 plants can vary between -21 and $-36^0/_{00}$. In contrast, C_4 land plants (grasses and sedges) have $\delta^{13}C$ values between -9 and $-17^0/_{00}$ (Tieszen et al. [1979]; O´Leary [1981], [1988]; Meyers [1990]; Collister et al. [1994]; Ficken et al. [2000]; Chikaraishi and Naraoka [2003]; Bi et al. [2005]), with a mean value of $-13^0/_{00}$. It has also been reported that bulk $\delta^{13}C$ values in gymnosperms are $3–6^0/_{00}$ higher than those of angiosperms (Chikaraishi and Naraoka [2003]; Stuiver and Braziunas [1987]). According to Brooks et al. ([1997]), the $\delta^{13}C$ values of evergreen trees are $3–4^0/_{00}$ higher than those of deciduous trees. Similarly, oak has $2–4^0/_{00}$ higher $\delta^{13}C$ values than pine (Williams and Ehleringer [1996]), although Huang et al. ([2006]) found that pine trees are $4–5^0/_{00}$ higher than oak trees.

Most C_4 species are grasses, belonging to Poaceae (40%) and sedges included in Cyperaceae family (15–20%) and are associated with warm and arid climates. Likewise, most Chenopodiaceae are C_4 plants. Moreover, gymnosperms do not use the C_4 photosynthetic pathway, and only 3% of angiosperms use this cycle for CO_2 fixation.

Crassulacean acid metabolism (CAM) is a less common C_3 pathway (Winter el al. 2005) used by plants mostly under certain environmental niches, e.g., desert succulents and tropical epiphytes (Keeley and Rundel 2003). Thus, CAM plants make a very low contribution to biomass and provide intermediate $\delta^{13}C$ values between those of C_3 and C_4 plants.

Freshwater phytoplankton typically has $\delta^{13}C$ values between -20 and $-30^0/_{00}$ (Galimov 1985). According to France (1995), the mean $\delta^{13}C$ value of phytopkankton is $-22^0/_{00}$, whereas algae is $-17^0/_{00}$. Aichner et al. (2010) reported values between -13.1 and $-16.8^0/_{00}$ in samples of the algae *Chara*.

The rapid decomposition of algae in comparison with land plants implies that there is little preservation of OM derived from phytoplankton and algae and that this material contributes only a low concentration of *n*-alkanes (Cranwell et al. 1987; Meyers 2003; Montagna and Ruber 1980).

Nevertheless, several additional factors can determine $\delta^{13}C$ values, namely the geochemistry of the water, the exchange of CO_2 with the atmosphere, the dissolved inorganic matter reservoir, and the carbon acquisition mechanisms (Håkansson 1985; McKenzie 1985). In fact, phytoplankton and dominant aquatic plants can sometimes enrich the ^{13}C of biomass when photosynthesis occurs under CO_2 limiting conditions (Hodell and Schelske 1998; Sharkey and Berry 1985). Thus, an active uptake of HCO_3^- rather than CO_2 can lead to a ^{13}C-enrichment of biomass (Bernasconi et al. 1997; Espie et al. 1991; Goericke et al. 1994; Hollander and Mckenzie 1991; Laws et al. 1998).

Aquatic macrophytes can be especially abundant in some lacustrine environments (Aichner et al. 2010; Ficken et al. 2000; Liu et al. 2013) and can therefore contribute a significant amount of organic carbon and medium-chain *n*-alkanes to sediments.

The bulk $\delta^{13}C$ values of aquatic macrophytes are usually within the range of C_3 plants, although the characteristics of the water mass (high pH, alkalinity, high CO_2 consumption, producing limited CO_2 availability) can lead to less negative $\delta^{13}C$ values (because of HCO_3^- assimilation), similar to those of C_4 plants (Prins and Elzenga 1989; Keely and Sandquist 1992). Aichner et al. (2010) reported bulk $\delta^{13}C$ values ranging from -5.8 to $18.1^0/_{00}$ in submerged aquatic macrophytes (in the range of $\delta^{13}C$ values for C_4 plants), and between -25.7 and $-26.4^0/_{00}$ for emergent macrophytes. Similarly, the aquatic macrophytes studied by Chikaraishi and Naraoka (2003) showed bulk $\delta^{13}C$ values of between -14.6 and $-16.5^0/_{00}$.

The small oscillations of $\delta^{13}C$ values, ranging between -27.0 and $-29.0^0/_{00}$ observed in most of the samples from the PB core may indicate a major input from C_3 plants. Such plants may have been either grasses or trees characteristic of areas with distinct precipitation rates. Furthermore, C_3 trees include a huge variety of species with diverse ecological

characteristics, although it appeared that most of the OM derived from angiosperms, as they usually have more depleted $\delta^{13}C$ than gymnosperms. Nevertheless, according to pollen data, there is an overwhelming presence of *Pinus* along the record (Torres et al. 2020), although there is evidence that gymnosperms produce very few *n*-alkanes relative to angiosperms (Diefendorf et al. 2011), and *Pinus* pollen can be largely overrepresented due to the air and water buoyancy linked to its enlarged sac wings. Moreover, in the PB, gymnosperms were located at higher elevations, far from the lacustrine/palustrine water body, with run-off input of water estimated to contribute only about 8% of the total (Cañada 1984). Consequently, changes in the water table in the peat bog were controlled indirectly by infiltration of water from the surrounding mountains (artesian waters), where accumulated snow during colder phases subsequently melted.

However, these $\delta^{13}C$ values may also be characteristic of aquatic macrophytes (Müller and Mathesius 1999). Therefore, samples of this group cannot be ascribed to a specific palaeoenvironmental event.

In the uppermost ca. 7 m, many samples indicated that the OM derived from algae and/or aquatic macrophytes and land plants, as ACL values were < 26, and *P*aq ranged mainly between 0.6 and 0.3. However, some variations of the $\delta^{13}C_{org}$ values between 7.8 and 4.5 m (30–11.5 cal ka BP), with a maximum difference of $5^0/_{00}$ (-23.3 to $-28.3^0/_{00}$), were especially marked. This finding may indicate a change in vegetation, but within C_3 plant species. However, variations in macrophytes could also explain this increase.

Samples with lower $\delta^{13}C$ values of bulk OM [(7.8–7.7 m (30–29 cal ka BP); 6.9–6.7 m (22–20 cal ka BP); 5.9–5.6 m (18–17 cal ka BP) and 4.6 m (12 cal ka BP)] coincided with predominant *n*-alkane chains of 31 carbon atoms, which are typical of grasses (Cranwell 1973), and C_{27} or C_{29} predominant *n*-alkanes, common to trees (Cranwell 1973). Of note, these intervals can be correlated with a marked increase in steppe plants and a significant decrease in xerophilous taxa (Torres et al. 2020) and a significant reduction of the percentage of C_{27} with respect to the sum $C_{27} + C_{29} + C_{31}$ (Ortiz et al. 2010), thereby indicating the occurrence of cold-dry phases.

5.2.2 Compound-specific $\delta^{13}C$ values

Individual carbon isotopic compositions of *n*-alkanes are shown in Fig. 3, showing some oscillations that differed in medium-chain relative to long-chain *n*-alkanes, which complement the information on $\delta^{13}C$ of bulk OM.

In general, the $\delta^{13}C$ values of medium- and short-chain *n*-alkanes are more negative than those of long-chain homologues (Sinninghe Damsté et al. 2011; Sun et al. 2013). However, in the Padul record, the $\delta^{13}C$ values of C_{29} to

C_{33} *n*-alkanes were more depleted than those of the C_{23} homologue.

On the whole, the carbon isotopic composition of *n*-alkanes in plants is more depleted (by 6–13$^0/_{00}$) than $\delta^{13}C$ of bulk OM (Bi et al. 2005; Chikaraishi and Naraoka 2003; Collister et al. 1994; Eley et al. 2016; Vogts et al. 2009). Similar to bulk OM isotopic composition, the $\delta^{13}C$ values of *n*-alkanes are more depleted in C_3 plants (*n*-alkanes C_{25} to n-C_{35} typically range from -26 to $-42^0/_{00}$) than in C_4 vegetation (-14 to $-26^0/_{00}$) (Bi et al. 2005; Castañeda et al. 2009; Chikaraishi and Naraoka 2003; Collister et al. 1994; Eley et al. 2016; Liu et al. 2015; Pedentchouk et al. 2008; Simoneit 1997; Vogts et al. 2009). Similarly, the $\delta^{13}C$ values of *n*-alkanes are lower in C_3 angiosperms ($-36.1 \pm 2.7^0/_{00}$) than in C_3 gymnosperms ($-31.6 \pm 1.7^0/_{00}$) (Chikaraishi and Naraoka, 2003; Pedentchouk et al. 2008).

According to Liu et al. (2015), C_{27} of aquatic macrophytes shows $\delta^{13}C$ values ranging from -15.1 to $-26.0^0/_{00}$, and C_{29} from -15.7 to $-26.7^0/_{00}$. In this regard, Aichner et al. (2010) reported that submerged macrophytes show wide ranges of *n*-alkane $\delta^{13}C$ values: -13.3 to $-29.9^0/_{00}$, whereas emergent macrophytes vary from -29.2 to $-34.5^0/_{00}$.

Furthermore, $\delta^{13}C$ values between *n*-alkane homologues are widely variable in a single plant, being typically less than $6^0/_{00}$ (Bi et al. 2005; Chikaraishi and Naraoka 2003; Collister et al. 1994; Conte et al. 2003; Diefendorf et al. 2011, 2015; Dungait et al. 2011; Eley et al. 2016; Vogts et al. 2009), although reaching as much as $16^0/_{00}$ in some cases (Aichner et al. 2010; Chikaraishi and Naraoka 2003). Therefore, it is necessary to be cautious when interpreting small variations in the isotopic compositions of individual compounds isolated from sedimentary environments (Collister et al. 1994).

Moreover, the $\delta^{13}C$ values of a single *n*-alkane homologue of a plant can vary in a given location under changing environmental conditions, i.e. $\delta^{13}C$ *n*-C_{27} alkane of the birch *Betula pendula* shows seasonal variations of ca. $3^0/_{00}$ (Pedentchouk et al. 2008). Variations for *n*-C_{27}, *n*-C_{29} and *n*-C_{31} alkanes have also been reported for some saltmarsh species.

The shifts in the $\delta^{13}C$ values of sedimentary leaf waxes may result not only from climate variables but also from temporal shifts in the distribution of vegetation, as well as from changes in the isotopic signatures of higher plants undergoing metabolic processes or subjected to environmental stress (Pedentchouk et al. 2008), or as a result of adaptation to salinity (Eley et al. 2016).

Thus, the relatively narrow range of $\delta^{13}C$ values limits the application of carbon isotope techniques. Moreover, given that plant species produce widely varying amounts of *n*-alkanes, further complexity is introduced when interpreting biomarker-based $\delta^{13}C$ reconstructions, as species may bias the sedimentary record to a greater or lower extent depending on the amount of alkyl lipids they produce (Eley et al. 2016). Nevertheless, these uncertainties do not affect the interpretation of overall trends, where relatively enriched (depleted) bulk and/or *n*-alkane $\delta^{13}C$ values indicate a decrease or increase in the input of C_3/C_4 plants (Castañeda and Shouten 2011).

Here we observed a certain correlation between the ACL index and bulk $\delta^{13}C$ logs of OM and C_{23} and C_{25} *n*-alkanes, with low oscillations between 34 and 7 m (180–25 ka), and generally lower ACL values when $\delta^{13}C$ signals increased. These findings indicate that changes in vegetation may affect these proxies. However, no correspondence was observed between the *P*aq index and $\delta^{13}C$ logs, thereby indicating considerable and almost constant presence of emergent macrophytes throughout the record and that other factors were responsible for changes in $\delta^{13}C$ values. Therefore, the *n*-alkane indices revealed the contribution of vegetation to the sedimentology of the PB. However, specific considerations could be made on the basis of $\delta^{13}C$ values.

Similarly, the bulk $\delta^{13}C$ log was comparable to those of C_{23}, C_{25} and C_{27} homologues, with lower correspondence with long-chain *n*-alkanes (Fig. 3). The multivariate analysis (Table 1) showed that the $\delta^{13}C$ values of C_{23}, C_{25} and C_{27} were the main contributors to the bulk $\delta^{13}C$ signal, as they showed significant correlation coefficients. Of note, the C_{27} $\delta^{13}C$ signal was influenced mostly by the input of both aquatic macrophytes and land plants, as the correlation coefficient between $\delta^{13}C_{27}$ and $\delta^{13}C_{23}$ (0.66) and between $\delta^{13}C_{27}$ and $\delta^{13}C_{31}$ (0.43) was significant.

In general, compound-specific $\delta^{13}C$ values reproduced the bulk $\delta^{13}C$ signal. However, the range of values of each component differed. Furthermore, small differences were

Table 1 Correlation coefficients between $\delta^{13}C$ values of bulk and even *n*-alkanes from C_{23} to C_{33}

	$\delta^{13}C_{25}$	$\delta^{13}C_{27}$	$\delta^{13}C_{29}$	$\delta^{13}C_{31}$	$\delta^{13}C_{33}$	$\delta^{13}C_{bulk}$
$\delta^{13}C_{23}$	0.70	0.66	0.49	0.35	0.35	0.54
$\delta^{13}C_{25}$		0.64	0.53	0.36	0.35	0.48
$\delta^{13}C_{27}$			0.65	0.43	0.33	0.53
$\delta^{13}C_{29}$				0.46	0.32	0.36
$\delta^{13}C_{31}$					0.40	0.26
$\delta^{13}C_{33}$						0.28

observed in the δ^{13}C values of long-chain n-alkanes (C_{31} and C_{33}) between the interval located at 39–34 m (220–180 ka) and the rest of the core. In contrast, large differences were detected in those of medium-chain homologues. Therefore, between 39 and 34 m (220–180 ka), the bulk δ^{13}C signal was influenced mainly by medium-chain alkanes, typically abundant in aquatic macrophytes. However, it must be considered that, in this interval, the n-alkane predominant chain and ACL values were interpreted in terms of higher inputs of algae and aquatic plants, with terrestrial plants predominating in only few samples. Moreover, the Paq index did not show a significant increase, thereby indicating that the contribution of aquatic macrophytes was similar to that of the previous interval. In our view, the environmental conditions of the water body were responsible for these oscillations, rather than changes in the characteristics of the vegetation.

Of note, some macrophytes take up isotopically heavier HCO_3^- when CO_2 is limited (Allen and Spence 1981; Keeley and Sandsquist 1992; Van der Berg et al. 2002). In this regard, the δ^{13}C value of HCO_3^- is ca. $10^0/_{00}$ higher than that of dissolved CO_2 (Mook et al. 1974; Prins and Elzenga 1989), thus producing a shift towards less negative δ^{13}C values. According to Aichner et al. (2010), limited CO_2 availability in alkaline and/or shallow lakes with a dense macrophyte population can lead to submerged macrophytes of a single species showing a wide range of bulk δ^{13}C values. Moreover, the isotopic fractionation during n-alkane biosynthesis in plants is enhanced with increasing chain length and when more ^{13}C-enriched carbon sources (like HCO_3) are assimilated. Some submerged aquatic macrophytes tend to increase the production of long-chain alkanes, especially in very shallow lakes where macrophytes are exposed during dry episodes.

In fact, it has been proposed that shifts towards higher δ^{13}C values in C_{23} and C_{25} alkanes, typical of macrophytes, are caused by limited CO_2 availability induced by water temperature, salinity, pH, enhanced productivity, low atmospheric pCO2, or stagnant barriers (Street-Perrot et al. 2004). Moreover, when environmental conditions lead to the partial emersion of macrophytes (drop in water level due to dry episodes, thereby increasing exposure to sunlight and air), these plants increase the biosynthesis of C_{25} and long-chain n-alkanes in favour of the C_{23} homologue (Aichner et al. 2010). Therefore, our results point to enhanced isotopic fractionation during lipid synthesis by aquatic macrophytes within MIS 7, leading to an increase in the bulk and n-alkane δ^{13}C values. The presence of marls in this interval (39–34 m; 220–180 ka) reinforced this hypothesis. In this case, ACL values decreased, and there was a significant and positive shift of δ^{13}C values in medium-chain homologues (C_{23} and C_{25}), at which aquatic macrophytes maximize. In contrast, long-chain n-alkanes, especially C_{29}, C_{31} and C_{33}, did not vary. In this regard, the pollen analysis of the PB

record revealed that this stage was characterized, in general, by Mediterranean-like conditions with increasing moisture (Fig. 4): high taxa diversity, with an increase in Mediterranean, Riparian, Hygrophilous and Mesophilous, and pollen from these taxa predominated over that from aquatics (Torres et al. 2020). In addition, some phases of increasing aridity occurred. Futhermore, in other long Southwestern European pollen records within the same climatic region, for example those of Valle di Castiglione (Follieri et al. 1988), the marine core ODP-976 (Sánchez-Goñi et al. 2008), and Villarquemado (Valero-Garcés et al. 2019), MIS7 was also characterized by a marked expansion of deciduous forest, although some short phases of increasing aridity were also identified within this stage (Fig. 4).

As occurred with the bulk δ^{13}C signal, the δ^{13}C values of C_{27}, C_{29}, C_{31} and C_{33} n-alkanes fell within the range of C_3 plants, but showed greater variability. Episodes with lower δ^{13}C values [(7.8–7.7 m (30–29 cal ka BP); 6.9–6.7 m (22–20 cal ka BP); 5.9–5.6 m (18–17 cal ka BP) and 4.6 m (12 cal ka BP)] could be attributed to an important input from angiosperms. We compared the palaeoenvironmental characteristics obtained from the profiles of δ^{13}C values of bulk and of C_{25} n-alkane in the PB with the relative percentage of C_{27} with respect to the sum $C_{27} + C_{29} + C_{31}$ obtained in the PB (Ortiz et al. 2010) and in the Fuentillejo maar record (Ortiz et al. 2013) (Fig. 4). The low % C_{27} values, which are linked the retreat of deciduous forest and thus to drier conditions, are correlated with the maxima values of δ^{13}C curves, which corresponded to colder and drier episodes. This increase in aridity during these events was also confirmed by pollen analysis data in Padul (Torres et al. 2020) and Fuentillejo (Vegas et al. 2008 2010), observing a considerable rise in steppe plants, whereas xerophilous plants decreased. Therefore, these episodes represented cold-dry phases, which caused the recession of temperate forests and the extension of grasses, which can be correlated with Heinrich Events 3, 2 and 1 (Last Glacial Maximum) and the Younger Dryas, respectively.

These findings are consistent with palynological data from other long Southwestern European pollen records such as those of marine cores drilled off the coast of Spain (ODP-976, Sánchez-Goñi et al. 2008), and the continental sequences of Villarquemado (Valero Garcés et al. 2019), and Valle di Castiglioni (Follieri et al. 1988), in which the Heinrich Events and the Younger Dryas are characterized by a contraction of temperate tree populations and the expansion of steppe vegetation. Likewise, low δ^{13}C values occur in some lakes as a result of organisms feeding on isotopically light methane-derived carbon (Jones and Grey 2011; Kankaala et al. 2006). In anoxic conditions, anaerobic respiration produces ^{13}C-depleted methane, which can cause a decrease in δ^{13}C of algae and aquatic macrophytes

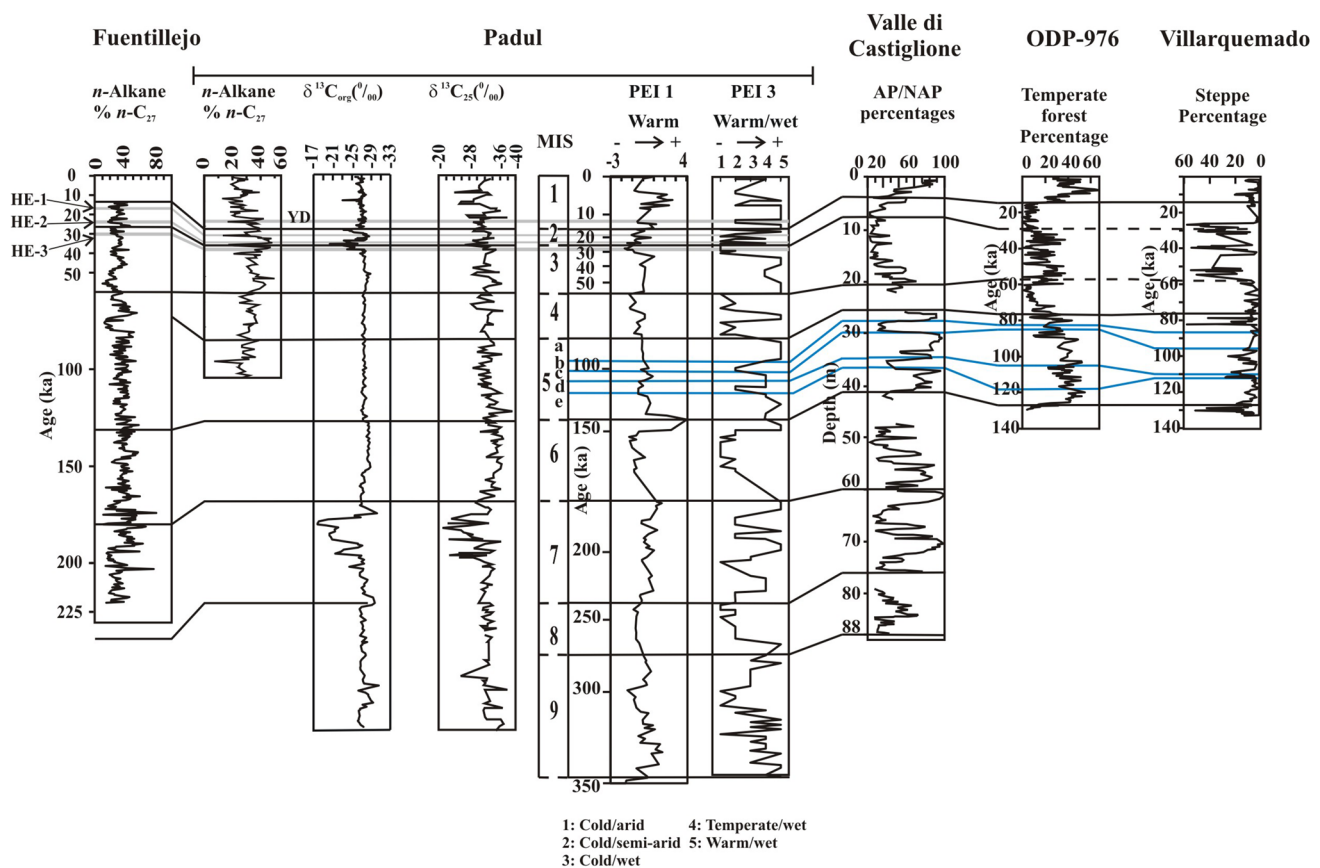**Fig. 4** Correlation between the profiles of $\delta^{13}C$ values of bulk and C_{25} n-alkane in the Padul Basin and the relative percentage of C_{27} with respect to the sum $C_{27}+C_{29}+C_{31}$ (a proxy for increasing deciduous tres and humidity) in Padul (Ortiz et al. 2010) and in Fuentillejo (Ortiz et al. 2013), the palaeoenvironmental conditions during MIS interpreted in Padul based on the pollen content (Torres et al. 2020) and those in the following long Southwestern Euro-

pean pollen records: Valle di Castiglione (Follieri et al. 1988); ODP-976 (Sánchez-Goñi et al. 2008), and Villarquemado (Valero-Garcés et al. 2019). *AP* arboreal pollen, *NAP* non-arboreal pollen. The pollen records were plotted in age or depth according to their original published source, and the correlation was performed according to the description of environmental episodes and MIS found in the original papers

(Holander and Smith 2001). This phenomenon is likely to have occurred in the PB, as the medium-chain components also showed significant variations, in some cases coinciding with those of long-chain homologues. However, this variability can be attributed mainly to changing environmental conditions (Pedentchouk et al. 2008), temporal shifts in the distribution of vegetation or environmental stress (Pedentchouk et al. 2008), as large $\delta^{13}C$ shifts occurred in long-chain homologues, which are typically abundant in terrestrial plants.

In the uppermost 7 m of the core (ca. 25 ka), the rise in $\delta^{13}C$ values in medium-chain components (C_{23} and C_{25}) could be attributed to an increase in the relative contribution of aquatic macrophytes to OM, as ACL values decreased and the *P*aq index increased. Likewise, the

uptake of heavier CO_2 from the water body may have occurred, leading to higher $\delta^{13}C$ values.

These results confirm that C_4 plants had a low presence in the PB during MIS7 as also observed in the pollen record (Torres et al. 2020). Therefore, the $\delta^{13}C$ logs were ideal for testing the influence of aquatic macrophytes on the lipid and isotopic composition of sediments. Coinciding with Liu et al. (2015), the $\delta^{13}C$ values of the C_{31} alkane was a reliable proxy for C_4/C_3 terrestrial vegetation composition in Lake Qinghai (Tibet Plateau), as emergent macrophytes made a minor contribution to this homologue. In contrast, the $\delta^{13}C$ values of C_{23} and C_{25} alkanes reflected mainly ecological conditions due to the large portion of these compounds in the aquatic macrophytes of this lake.

6 Conclusions

The *n*-alkane content, and $\delta^{13}C$ values of these lipids and of bulk OM allowed us to infer the palaeoenvironmental conditions of the PB in the last 320 ka. The $\delta^{13}C$ signal of long-chain *n*-alkanes was a reliable proxy for C_4 and C_3 plant content in the basin, as emergent macrophytes made a minor contribution to these homologues. Episodes with depleted $\delta^{13}C$ values were linked to a significant contribution of plants using the C_3 photosynthetic pathway, with the lowest $\delta^{13}C$ values indicating a considerable input of angiosperms, linked to cold and dry conditions. Of note, these values could also be attributed to changing environmental conditions or environmental stress, as important shifts in $\delta^{13}C$ occurred in long-chain homologues, which are typically abundant in terrestrial plants.

In contrast, the $\delta^{13}C$ values of medium-chain alkanes (C_{23} and C_{25}) reflected mainly the ecological conditions of the lake since the aquatic macrophytes of this water body contained a large portion of these compounds. The shifts in $\delta^{13}C$ of these homologues were attributed to limited CO_2 availability induced by water temperature, salinity, pH, enhanced productivity, low atmospheric pCO_2, or stagnant barriers, rather than the abundance of aquatic macrophytes. The $\delta^{13}C$ values of *n*-alkanes and of bulk OM did not show significant variations and therefore were not greatly affected by palaeoenvironmental variations. In contrast, our results point to enhanced isotopic fractionation during lipid synthesis by aquatic macrophytes (and/or algae) within MIS 7 and the Holocene, which led to increased bulk OM and *n*-alkane $\delta^{13}C$ values. In coherence with biomarker analysis and pollen data of the PB and other Southwestern Mediterranean records, these proxies indicated that MIS 7 was characterized by increasing moisture. Furthermore, some episodes belonging to MIS 2 and 1 with lower *n*-alkane $\delta^{13}C$ values were attributed to cold-dry episodes (Heinrich Events 3, 2, 1 and Younger Dryas). Therefore, general global climatic oscillations that occurred during these stages appear to have also influenced the environmental conditions in southern Spain. Similar findings were obtained for the biomarker analysis for the PB record (Ortiz et al. 2010), located in southern Spain. The $\delta^{13}C$ logs were, therefore, ideal for testing the influence of aquatic macrophytes on the lipid and isotopic composition of the sediments. Our results confirm that C_4 plants were not abundant in the PB during MIS 7.

References

Aichner, B., Herzschuh, U., & Wilkes, H. (2010). Influence of aquatic macrophytes on the stable carbon isotopic signatures of sedimentary organic matter in lakes on the Tibetan Plateau. *Organic Geochemistry, 41*, 706–718.

Alfaro, P., López-Garrido, A. C., Galindo-Zaldívar, J., Sanz de Galdeano, C., & Jabaloy, A. (2001). Evidence for the activity and paleoseismicity of the Padul fault (Betic Cordillera, southern Spain). *Acta Geológica Hispánica, 36*, 283–295.

Allen, E. D., & Spence, D. H. N. (1981). The differential ability of aquatic plants to utilize the inorganic carbon supply in fresh water. *New Phytologist, 87*, 269–283.

Bernasconi, S. M., Barbieri, A., & Simona, M. (1997). Carbon and nitrogen isotope variations in sedimenting organic matter in Lake Lugano. *Limnology and Oceanography, 42*, 1755–1765.

Bi, X., Sheng, G., Liu, X., Li, C., & Fu, J. (2005). Molecular and carbon and hydrogen isotopic composition of *n*-alkanes in plant leaf waxes. *Organic Geochemistry, 36*, 1405–1417.

Blaauw, M., & Christen, J. A. (2011). Flexible paleoclimate age-depth models using an autoregressive gamma process. *Bayesian Analysis, 6*, 457–474.

Blumer, M., Guillard, R. R. L., & Chase, T. (1971). Hydrocarbons of marine plankton. *Marine Biology, 8*, 183–189.

Brenner, M., Whitmore, T. J., Curtis, J. H., Hodell, D. A., & Schelske, C. L. (1999). Stable isotope ($\delta^{13}C$ and $\delta^{15}N$) signatures of sedimented organic matter as indicators of historic lake trophic state. *Journal of Paleolimnology, 22*, 205–221.

Brooks, J. R., Flanagan, L. B., Buchmann, N., & Ehleringer, J. R. (1997). Carbon isotope composition of boreal plants: functional grouping of life forms. *Oecologia, 110*, 301–311.

Bush, R. T., & McInerney, F. A. (2013). Leaf wax *n*-alkane distributions in and across modern plants: implications for paleoecology and chemotaxonomy. *Geochimica Et Cosmochimica Acta, 117*, 161–179.

Bush, R. T., & McInerney, F. A. (2015). Influence of temperature and C^4 abundance on *n*-alkane chain length distributions across the central USA. *Organic Geochemistry, 79*, 65–73.

Camuera, J., Jiménez-Moreno, G., Ramos-Román, M. J., García-Alix, A., Toney, J. L., Anderson, R. S., et al. (2018). Orbital-scale environmental and climatic changes recorded in a new ~200,000-year-long multiproxy sedimentary record from Padul, southern Iberian Peninsula. *Quaternary Science Reviews, 198*, 91–114.

Camuera, J., Jiménez-Moreno, G., Ramos-Román, M. J., García-Alix, A., Toney, J. L., Anderson, R. S., et al. (2019). Vegetation and

climate changes during the last two glacial-interglacial cycles in the western Mediterranean: a new long pollen record from Padul (southern Iberian Peninsula). *Quaternary Science Reviews, 205*, 86–105.

Cañada, P. (1984). Estudio hidrogeológico preliminar y de drenaje de las explotaciones a cielo abierto de lignito de Arenas del Rey y de turba de Padul. M. thesis, Granada University, 189 pp.

Castañeda, I. S., & Schouten, S. (2011). A review of molecular organic proxies for examining modern and ancient lacustrine environments. *Quaternary Science Reviews, 30*, 2851–2891.

Castañeda, I. S., Mulitza, S., Schefuß, E., Lopes dos Santos, R. A., Sinninghe Damsté, J. S., & Schouten, S. (2009). Wet phases in the Sahara/Sahel region and human migration patterns in North Africa. *Proceedings of the National Academy of Sciences, 106*(48), 20159–20163.

Cerling, T. E., Harris, J. M., MacFadden, B. J., Leakey, M. G., Quade, J., Eisenmann, V., & Ehleringer, J. (1997). Global vegetation change through the Miocene/Pliocene boundary. *Nature, 389*, 153–158.

Chikaraishi, Y., & Naraoka, H. (2003). Compound-specific δD–$\delta^{13}C$ analyses of *n*-alkanes extracted from terrestrial and aquatic plants. *Phytochemistry, 63*, 361–371.

Collister, J. W., Rieley, G., Stern, B., Eglinton, J., & Fry, B. (1994). Compound-specific $\delta^{13}C$ analyses of leaf lipids from plants with differing carbon dioxide metabolisms. *Organic Geochemistry, 21*, 619–627.

Conte, M. H., Weber, J. C., Carlson, P. J., & Flanagan, L. B. (2003). Molecular and carbon isotopic composition of leaf wax in vegetation and aerosols in a northern prairie ecosystem. *Oecologia, 135*, 67–77.

Cranwell, P. A. (1973). Chain-length distribution of *n*-alkanes from lake sediments in relation to postglacial environmental change. *Freshwater Biology, 3*, 259–265.

Cranwell, P. A. (1984). Lipid geochemistry of sediments from Upton Broad, a small productive lake. *Organic Geochemistry, 7*, 25–37.

Cranwell, P. A., Eglinton, G., & Robinson, N. (1987). Lipids of aquatic organisms as potential constributors to lacustrine sediments-II. *Organic Geochemistry, 11*, 513–527.

Diefendorf, A. F., Mueller, K. E., Wing, S. L., Koch, P. L., & Freeman, K. H. (2010). Global patterns in leaf 13C discrimination and implications for studies of past and future climate. *Proceedings of the National Academy of Sciences of the United States of America, 107*, 5738–5743.

Diefendorf, A. F., Freeman, K. H., Wing, S. L., & Graham, H. V. (2011). Production of *n*-alkyl lipids in living plants and implications for the geologic past. *Geochimica Et Cosmochimica Acta, 75*, 7472–7485.

Diefendorf, A. F., Leslie, A. B., & Wing, S. L. (2015). Leaf wax composition and carbon isotopes vary among major conifer groups. *Geochimica Et Cosmochimica Acta, 170*, 145–156.

Dungait, J. A., Docherty, G., Straker, V., & Evershed, R. P. (2011). Variation in bulk tissue, fatty acid and monosaccharide $\delta^{13}C$ values between autotrophic and heterotrophic plant organs. *Phytochemistry, 72*, 2130–2138.

Eglinton, G., & Calvin, M. (1967). Chemical fossils. *Scientific American, 216*, 32–43.

Eglinton, G., & Hamilton, R. J. (1963). The distribution of *n*-alkanes. In T. Swain (Ed.), *Chemical Plant Taxonomy* (pp. 87–217). Academic Press.

Eglinton, G., & Hamilton, R. J. (1967). Leaf epicuticular waxes. *Science, 156*, 1322–1335.

Eley, Y., Dawson, L., & Pedentchouk, N. (2016). Investigating the carbon isotope composition and leaf wax *n*-alkane concentration of C_3 and C_4 plants in Stiffkey saltmarsh, Norfolk, UK. *Organic Geochemistry, 96*, 28–42.

Espie, G. S., Miller, G. A., Kandasamy, R. A., & Cavin, D. T. (1991). Active HCO_3^- transport in cyanobacteria. *Canadian Journal of Botany, 69*, 936–944.

Farquhar, G. D., Ehleringer, J. R., & Hubick, K. T. (1989). Carbon isotope discrimination and photosynthesis. *Annual Review of Plant Biology, 40*, 503–537.

Ficken, K. J., Street-Perrott, F. A., Perrott, R. A., Swain, D. L., Olago, D. O., & Eglinton, G. (1998). Glacial/interglacial variations in carbon cycling revealed by molecular and isotope stratigraphy of Lake Nkunga, Mt. Kenya East Africa. *Organic Geochemistry, 29*, 1701–1719.

Ficken, K. J., Li, B., Swain, D. L., & Eglinton, G. (2000). An *n*-alkane proxy for the sedimentary input of submerged/floating freshwater aquatic macrophytes. *Organic Geochemistry, 31*, 745–749.

Florschütz, F., Menéndez Amor, J., & Wijmstra, T. A. (1971). Palinology of a thick Quaternary succession in southern Spain. *Palaeogeography, Palaeoclimatology, Palaeoecology, 10*, 233–264.

Follieri, M., Magri, D., & Sadori, L. (1988). 250,000-year pollen record from Valle di Castiglione (Roma). *Pollen Spores, 3–4*, 329–356.

France, R. L. (1995). C-13 Enrichment in benthic compared to planktonic algae—Foodweb implications. *Marine Ecology Progress Series, 124*, 307–317.

Gelpi, E., Scheider, H., Mann, J., & Oro, J. (1970). Hydrocarbons of geochemical significance in microscopic algae. *Phytochemistry, 9*, 603–612.

Goericke, J. P., Montoya, J. P., & Fry, B. (1994). Physiology of isotopic fractionation in algae and cyanobacteria. In K. Lajtha & R. H. Michener (Eds.), *Stable Isotopes in Ecology and Environmental Science* (pp. 187–221). Blackwell.

Håkansson, S. (1985). A review of various factors influencing the stable carbon isotope ratio of organic lake sediments by the change from Glacial to post-Glacial environmental conditions. *Quaternary Science Reviews, 4*, 135–146.

Hodell, D. A., & Schelske, C. L. (1998). Production, sedimentation, and isotopic composition of organic matter in Lake Ontario. *Limnology and Oceanography, 43*, 200–214.

Hollander, D. J., & Mckenzie, J. A. (1991). CO_2 control on carbon-isotope fractionation during aqueous photosynthesis: a paleo-pCO_2 barometer. *Geology, 19*, 929–932.

Hollander, D. J., & Smith, M. A. (2001). Microbially mediated carbon cycling as a control on the $\delta^{13}C$ of sedimentary carbon in eutrophic Lake Mendota (USA): new models for interpreting isotopic excursions in the sedimentary record. *Geochimica Et Cosmochimica Acta, 65*, 4321–4337.

Hollander, D. J., Mckenzie, J. A., & Lo ten Haven, H. (1992). A 200 year sedimentary record of progressive eutrophication in lake Greifen (Switzerland): implications for the origin of organic-carbon-rich sediments. *Geology, 20*, 825–828.

Huang, Y., Dupont, L., Sarnthein, M., Hayes, J. M., & Eglinton, G. (2000). Mapping of C4 plant input from North West Africa into North East Atlantic sediments. *Geochimica Et Cosmochimica Acta, 64*, 3505–3513.

Huang, Y., Street-Perrott, F. A., Metcalfe, S. E., Brenner, M., Moreland, M., & Freeman, K. (2001). Climate change as the dominant control on glacial-interglacial variations in C_3 and C_4 plant abundance. *Science, 293*, 1647–1651.

Huang, Y., Shuman, B., Wang, Y., Webb, T., Grimm, E. C., & Jacobson, G. L. (2006). Climatic and environmental controls on the variation of C_3 and C_4 plant abundances in central Florida for the past 62,000 years. *Palaeogeography, Palaeoclimatology, Palaeoecology, 237*, 428–435.

Jones, R. I., & Grey, J. (2011). Biogenic methane in freshwater food webs. *Freshwater Biology, 56*, 213–229.

Kankaala, P., Taipale, S., Grey, J., Sonninen, E., Arvola, L., & Jones, R. I. (2006). Experimental $\delta^{13}C$ evidence for a contribution of

methane to pelagic food webs in lakes. *Limnology and Oceanography, 51*, 2821–2827.

Keeley, J. E., & Rundel, P. P. (2003). Evolution of CAM and C[4] carbon-concentrating mechanism. *International Journal of Plant Sciences, 164*, 55–77.

Keely, J. E., & Sandsquist, D. R. (1992). Carbon: freshwater plants. *Plant and Cell Environment, 15*, 1021–1035.

Laws, E. A., Thompson, P. A., Popp, B. N., & Bidigare, R. R. (1998). Sources of inorganic carbon for marine microalgal photosynthesis: a reassessment of $\delta^{13}C$ data from batch culture studies of *Thalassiosira pseudonana* and *Emiliana huxleyi*. *Limnology and Oceanography, 43*, 136–142.

Liu, W., Li, X., An, Z., Xu, L., & Zhang, Q. (2013). Total organic carbon isotopes: a novel proxy of lake level from Lake Qinghai in the Qinghai-Tibet Plateau, China. *Chemical Geology, 347*, 153–160.

Liu, W., Yang, H., Wang, H., An, Z., Wang, Z., & Leng, Q. (2015). Carbon isotope composition of long chain leaf wax *n*-alkanes in lake sediments: a dual indicator of paleoenvironment in the Qinghai-Tibet Plateau. *Organic Geochemistry, 83–84*, 190–201.

Lucini, M., Torres, T., Llamas, J. F., Canoira, L., Ortiz, J. E., & García de la Morena, M. A. (2000). Geoquímica orgánica de las lutitas lacustres de las cuencas cenozoicas del Duero y Ebro. *Geogaceta, 28*, 93–96.

Mckenzie, J. A. (1985). Carbon isotopes and productivity in the lacustrine and marine environments. In W. Stumm (Ed.), *Chemical Processes in Lakes* (pp. 99–118). Wiley.

Menéndez Amor, J., & Florschütz, F. (1962). Un aspect de la végétation en Espagne méridionale durant la dernière glaciation et l´Holocène. *Geology in Mijnbouw, 41*, 131–134.

Menéndez Amor, J., & Florschütz, F. (1964). Results of the preliminary palynological investigation of samples from a 50 m boring in southern Spain. B*oletín de la Real Sociedad Española de Historia Natural (Geología), 62*, 251–255.

Meyers, P. A. (1990). Impacts of regional Late quaternary climate changes on the deposition of sedimentary organic matter in Walker Lake Nevada. *Palaeogeography, Palaeoclimatology, Palaeoecology, 78*, 229–240.

Meyers, P. A. (1997). Organic geochemical proxies of paleoceanographic, paleolimnologic, and paleoclimatic processes. *Organic Geochemistry, 27*, 213–250.

Meyers, P. A. (2003). Applications of organic geochemistry to paleolimnological reconstructions: a summary of examples from the Laurentian Great Lakes. *Organic Geochemistry, 34*, 261–289.

Meyers, P. A., & Ishiwatari, R. (1993). Lacustrine organic geochemistry—an overview of indicators of organic matter sources and diagenesis in lake sediments. *Organic Geochemistry, 20*, 867–900.

Meyers, P. A., & Lallier-Verges, E. (1999). Lacustrine sedimentary organic matter records of late quaternary paleoclimates. *Journal of Paleolimnology, 21*, 345–372.

Meyers, P. A., Leenheer, M. J., & Bourbonniere, R. A. (1995). Diagenesis of vascular plant organic matter components during burial in lake sediments. *Aquatic Geochemistry, 1*, 35–42.

Montagna, P., & Ruber, E. (1980). Decomposition of *Spartina alterniflora* in different seasons and habitats of a northern Massachusetts salt marsh, and a comparison with other Atlantic regions. *Estuaries, 56*, 1859–1861.

Mook, W. G., Bommerson, J. C., & Staverman, W. H. (1974). Carbon isotope fractionation between dissolved bicarbonate and gaseous carbon dioxide. *Earth and Planetary Science Letters, 22*, 169–176.

Müller, A., & Mathesius, U. (1999). The palaeoenvironments of coastal lagoons in the southern Baltic Sea. The application of sedimentary C_{org}/N ratios as source indicators of organic matter. *Palaeogeography, Palaeoclimatology, Palaeoecology, 145*, 1–16.

Nestares, T., & Torres, T. (1998). Un nuevo sondeo de investigación paleoambiental del Pleistoceno y Holoceno en la turbera de Padul (Granada, Andalucía). *Geogaceta, 23*, 99–102.

Nott, C. J., Xie, S., Avsejs, L. A., Maddy, D., Chambers, F. M., & Evershed, R. P. (2000). N- alkane distribution in ombrotrophic mires as indicators of vegetation change related to climatic variation. *Organic Geochemistry, 31*, 231–235.

O'Leary, M. H. (1981). Carbon isotopic fractionation in plants. *Phytochemistry, 20*, 553–567.

O'Leary, M. H. (1988). Carbon isotopes in photosynthesis. Fractionation techniques may reveal new aspects of carbon dynamic in plants. *BioScience, 38*, 328–329.

Ogura, K., Machilara, T., & Takada, H. (1990). Diagenesis of biomarkers in Biwa lake sediments over 1 million years. *Organic Geochemistry, 16*, 805–813.

Ortiz, J. E., Torres, T., Delgado, A., Julià, R., Lucini, M., Llamas, F. J., Reyes, E., Soler, V., & Valle, M. (2004). The palaeoenvironmental and palaeohydrological evolution of Padul Peat Bog (Granada, Spain) over one million years, from elemental, isotopic, and molecular organic geochemical proxies. *Organic Geochemistry, 35*, 1243–1260.

Ortiz, J. E., Torres, T., Delgado, A., Llamas, F. J., & Valle, M. (2010). Palaeoenvironmental changes in the Padul Basin (Granada, Spain) over the last 1 Ma B.P. based on the biomarker content. *Palaeogeography, Palaeoclimatology, Palaeoecology, 298*, 286–299.

Ortiz, J. E., Moreno, L., Torres, T., Vegas, J., Ruiz-Zapata, B., García-Cortés, A., Galán, L., & Pérez-González, A. (2013). 220-ka palaeoenvironmental reconstruction of the Fuentillejo maar lake record (Central Spain) using biomarker analysis. *Organic Geochemistry, 55*, 85–97.

Pancost, R. D., Baas, M., van Geel, B., & Sinninghe Damsté, J. S. (2002). Biomarkers as proxies for plant inputs to peats: an example from a sub-boreal ombrotrophic bog. *Organic Geochemistry, 33*, 675–690.

Pedentchouk, N., Sumner, W., Tipple, B., & Pagani, M. (2008). $\delta^{13}C$ and δD compositions of *n*-alkanes from modern angiosperms and conifers: an experimental set up in central Washington state, USA. *Organic Geochemistry, 39*, 1066–1071.

Pons, A., & Reille, M. (1988). The Holocene and upper Pleistocene pollen record from Padul (Granada, Spain): a new study. *Palaeogeography, Palaeoclimatology, Palaeoecology, 66*, 243–263.

Poynter, J.G. (1989). Molecular stratigraphy: the recognition of Palaeoclimatic signals in organic geochemical data (Ph.D. thesis). University of Bristol, 240 pp.

Prins, H. B. A., & Elzenga, J. T. M. (1989). Bicarbonate utilization: function and mechanism. *Aquatic Botany, 34*, 59–83.

Ramos-Román, M. J., Jiménez-Moreno, G., Camuera, J., García-Alix, A., Anderson, R. C., Jiménez-Espejo, F. J., & Carrión, J. S. (2018a). Holocene climate aridification trend and human impact interrupted by millennial- and centennial-scale climate fluctuations from a new sedimentary record from Padul (Sierra Nevada, southern Iberian Peninsula). *Climate of the past, 14*, 117–137.

Ramos-Román, M. J., Jiménez-Moreno, G., Camuera, J., García-Alix, A., Scott Anderson, R., Jiménez-Espejo, F. J., Sachse, D., Toney, J. L., Carrión, J. S., Webster, C., & Yanes, Y. (2018b). Millennial-scale cyclical environment and climate variability during the Holocene in the western Mediterranean region deduced from a new multi-proxy analysis from the Padul record (Sierra Nevada, Spain). *Global and Planetary Change, 168*, 35–53.

Rieley, G., Collier, R. J., Jones, D. M., & Eglinton, G. (1991). The biogeochemistry of Ellesmere Lake, U.K.-I: source correlation of leaf wax inputs to the sedimentary record. *Organic Geochemistry, 17*, 901–912.

Rivas-Martínez, S. (1987). Memoria del mapa de Series de Vegetación de España, 1:400.000. Ministerio de Agricultura, Pesca y Alimentación, ICONA, Madrid.

Rivas-Martínez, S., & Rivas-Sáenz, S. (2009). Worldwide bioclimatic classification system. www.globalbioclimatics.org Accessed 15 September 2018.

Rommerskirchen, F., Eglington, G., Dupont, L., Günter, U., Wenzel, C., & Rullkötter, J. (2003). A north to south transect of Holocene southeast Atlantic continental margin sediments: relationship between aerosol transport and compound-specific δ^{13}C land plant biomarker and pollen records. *Geochemistry, Geophysics, Geosystems, 4*, 1101.

Sánchez-Castillo, P. M., & Morales-Torres, C. (1981). Algunas especies higrofíticas de la provincia de Granada. *Annales Del Jardín Botánico De Madrid, 37*, 677–692.

Sánchez-Goñi, M. F., Landais, A., Fletcher, W. J., Naughton, F., Desprat, S., & Duprat, J. (2008). Contrasting impacts of Dansgaard-Oeschger events over a western European latitudinal transect modulated by orbital parameters. *Quaternary Science Reviews, 27*, 1136–1151.

Schwark, L., Zink, K., & Lechterbeck, J. (2002). Reconstruction of postglacial to early Holocene vegetation history in terrestrial Central Europe via cuticular lipid biomarkers and pollen records from lake sediments. *Geology, 30*, 463–466.

Seki, O., Nakatsuka, T., Shibata, H., & Kawamura, K. (2010). A compound-specific *n*-alkane δ^{13}C and δD approach for assessing source and delivery processes of terrestrial organic matter within a forested watershed in northern Japan. *Geochimica Et Cosmochimica Acta, 74*, 599–613.

Sharkey, T. D., & Berry, J. A. (1985). Carbon isotope fractionation of algae as influenced by an inducible CO_2 concentrating mechanism. In W. J. Lucas & J. A. Berry (Eds.), *Inorganic Carbon Uptake by Aquatic Photosynthetic Organisms* (pp. 389–401). American Society of Plant Physiology.

Simoneit, B. R. T. (1997). Compound-specific carbon isotope analyses of individual long-chain alkanes and alkanoic acid in Harmattan aerosols. *Atmospheric Environment, 31*, 2225–2233.

Sinninghe Damsté, J. S., Verschuren, D., Ossebaar, J., Blokker, J., van Houten, R., van der Meer, M. T. J., Plessen, B., & Schouten, S. (2011). A 25,000-year record of climate-induced changes in lowland vegetation of eastern equatorial Africa revealed by the stable carbon-isotopic composition of fossil plant leaf waxes. *Earth and Planetary Science Letters, 302*, 236–246.

Street-Perrott, F. A., Huang, Y., Perrott, R. A., Eglinton, G., Barker, P., Ben Khelifa, L., Harkness, D. D., & Olago, D. (1997). Impact of lower atmospheric CO_2 on tropical mountain ecosystems: carbon-isotope evidence. *Science, 278*, 1422–1426.

Street-Perrott, F. A., Ficken, K. J., Huang, Y., & Eglinton, G. E. (2004). Late quaternary changes in carbon cycling on Mt. Kenya, East Africa: an overview of the δ^{13}C record in lacustrine organic matter. *Quaternary Science Reviews, 23*, 861–879.

Stuiver, M., & Braziunas, T. F. (1987). Tree cellulose ^{13}C/^{12}C isotope ratios and climate change. *Nature, 328*, 58–60.

Sun, Q., Xie, M., Shi, L., Zhang, Z., Lin, Y., Shang, W., Wang, K., Li, W., Liu, J., & Chu, G. (2013). Alkanes, compound-specific carbon isotope measures and climate variation during the last millennium from varved sediments of Lake Xiaolongwan, northeast China. *Journal of Paleolimnology, 50*, 331–344.

Talbot, M. R., & Johannessen, T. (1992). A high resolution palaeoclimatic record for the last 27,500 years in tropical West Africa from the carbon and nitrogen isotopic composition of lacustrine organic matter. *Earth and Planetary Science Letters, 110*, 23–37.

Teranes, J. L., & Bernasconi, S. M. (2005). Factors controlling d13C values of sedimentary carbon in hypertrophic Baldeggersee, Switzerland, and implications for interpreting isotope excursions in lake sedimentary records. *Limnology and Oceanography, 50*, 914–922.

Tieszen, L. L., Senyimba, M. M., Imbamba, S. K., & Troughton, J. H. (1979). The distribution of C_3 and C_4 grasses and carbon isotope discrimination along an altitudinal and moisture gradient in Kenya. *Oecologia, 37*, 337–350.

Torres, T., Valle, M., Ortiz, J. E., Soler, V., Araujo, R., Rivas, M. R., Delgado, A., Julià, R., & Sánchez-Palencia, Y. (2020). 800 ka of palaeoenvironmental changes in the Southwestern Mediterranean realm. *Journal of Iberian Geology, 46*, 117–144.

Valero-Garcés, B. L., González-Sampériz, P., Gil Romera, G., Benito, B. M., Moreno, A., Oliva-Urcia, B., Aranbarri, J., García-Prieto, E., Frugone, M., Morellón, M., Arnold, L. J., Demuro, M., Hardiman, M., Blockley, S. P. E., & Lane, C. S. (2019). A multi-dating approach to age-modelling long continental records: The 135 ka El Cañizar de Villarquemado sequence (NE Spain). *Quaternary Geochronology, 54*, 101006.

Van den Berg, M., Coops, H., Simons, J., & Pilon, J. (2002). A comparative study of the use of inorganic carbon resources by *Chara aspera* and *Potamogeton pectinatus*. *Aquatic Botany, 72*, 219–233.

Vegas, J., Ruiz-Zapata, B., Ortiz, J. E., Galán, L., Torres, T., García-Cortés, A., Pérez-González, A., & Gallardo-Millán, J. L. (2008). Identificación de las principales fases áridas del Pleistoceno superior en el registro sedimentario lacustre del maar de Fuentillejo (Campo de Calatrava). *Geo-Temas, 10*, 1467–1470.

Vegas, J., Ruiz-Zapata, B., Ortiz, J. E., Galán, L., Torres, T., García-Cortés, A., Gil-García, M. J., Pérez-González, A., & Gallardo-Millán, J. L. (2010). Identification of arid phases during the last 50 kyr cal BP from the Fuentillejo maar lacustrine record (Campo de Calatrava Volcanic Field, Spain). *Journal of Quaternary Science, 25*, 1051–1062.

Viso, A. C., Pesando, D., Bernard, P., & Marty, J. C. (1993). Lipids components of the Mediterranean seagrass *Posidonea oceanica*. *Phytochemistry, 34*, 381–387.

Vogts, A., Moossen, H., Rommerskirchen, F., & Rullkötter, J. (2009). Distribution patterns and stable carbon isotopic composition of alkanes and alkan-1-ols from plant waxes of African rain forest and savanna C_3 species. *Organic Geochemistry, 40*, 1037–1054.

Williams, D. G., & Ehleringer, J. R. (1996). Carbon isotope discrimination in three semi-arid woodland species along a monsoon gradient. *Oecologia, 106*, 455–460.

Winter, K., Aranda, J., & Holtum, J. A. M. (2005). Carbon isotope composition and water-use efficiency in plants with crassulacean acid metabolism. *Functional Plant Biology, 32*, 381–388.

Wolfe, B. B., Edwards, T. W. D., Beuning, K. R. M., & Elgood, R. J. (2001). Carbon and oxygen isotope analysis of lake sediment cellulose: Methods and applications. In W. M. Last & J. P. Smol (Eds.), *Tracking Environmental Changes Using Lake Sediments: Physical and Chemical Techniques* (pp. 373–400). Kluwer.

Xie, S., Guo, J., Huang, J., Chen, F., Wang, H., & Farrimond, P. (2004). Restricted utility of δ^{13}C of bulk organic matter as a record of paleovegetation in some loess–paleosol sequences in the Chinese Loess Plateau. *Quaternary Research, 62*, 86–93.

Yamamoto, S., Kawamura, K., Seki, O., Meyers, P. A., Zheng, Y., & Zhou, W. (2010). Environmental influences over the last 16ka on compound-specific δ^{13}C variations of leaf wax *n*-alkanes in the Hani peat deposit from northeast China. *Chemical Geology, 227*, 261–268.

Zhou, W., Xie, S., Meyers, P. A., & Zheng, Y. (2005). Reconstruction of late glacial and Holocene climate evolution in southern China from geolipids and pollen in the Dingnan peat sequence. *Organic Geochemistry, 36*, 1272–1284.